

Opportunities with top quarks at future circular colliders

Benjamin Fuks

CERN, PH-TH, CH-1211 Geneva 23, Switzerland

Institut Pluridisciplinaire Hubert Curien/Département Recherches Subatomiques, Université de Strasbourg/CNRS-IN2P3, 23 rue du Loess, F-67037 Strasbourg, France

E-mail: benjamin.fuks@iphc.cnrs.fr

Abstract. We describe various studies relevant for top physics at future circular collider projects currently under discussion. We show how highly-massive top-antitop systems produced in proton-proton collisions at a center-of-mass energy of 100 TeV could be observed and employed for constraining top dipole moments, investigate the reach of future proton-proton and electron-positron machines to top flavor-changing neutral interactions, and discuss top parton densities.

1. A future circular collider facility at CERN

The Large Hadron Collider (LHC) at CERN has delivered very high quality results during its first run in 2009-2013, with in particular the discovery of a Higgs boson with a mass of about 125 GeV in 2012. Unfortunately, no hint for the presence of particles beyond the Standard Model has been observed. Deviations from the Standard Model are however still allowed and expected to show up either through precision measurements of indirect probes, or directly at collider experiments. In this context, high precision would require to push the intensity frontier further and further, whereas bringing the energy frontier beyond the LHC regime would provide handles on new kinematical thresholds. Along these lines, a design study for a new accelerator facility aimed to operate at CERN in the post-LHC era has been undertaken. This study focuses on a machine that could collide protons at a center-of-mass energy of $\sqrt{s} = 100$ TeV, that could be built in a tunnel of about 80-100 km in the area of Geneva and benefit from the existing infrastructure at CERN [1]. A possible intermediate step in this project could include an electron-positron machine with a collision center-of-mass energy ranging from 90 GeV (the Z -pole) to 350 GeV (the top-antitop threshold), with additional working points at $\sqrt{s} = 160$ GeV (the W -boson pair production threshold) and 240 GeV (a Higgs factory) [2]. In parallel, highly-energetic lepton-hadron and heavy ion collisions are also under investigation.

Both the above-mentioned future circular collider (FCC) setups are expected to deliver a copious amount of top quarks. More precisely, one trillion of them are expected to be produced in 10 ab^{-1} of proton-proton collisions at $\sqrt{s} = 100$ TeV and five millions of them in the same amount of electron-positron collisions at $\sqrt{s} = 350$ GeV (which will in particular allows for top mass and width measurements at an accuracy of about 10 MeV [3]). This consequently opens the door for an exploration of the properties of the top quark, widely considered as a sensitive probe to new physics given its mass close to the electroweak scale, with an unprecedented accuracy. This is illustrated below with three selected examples.

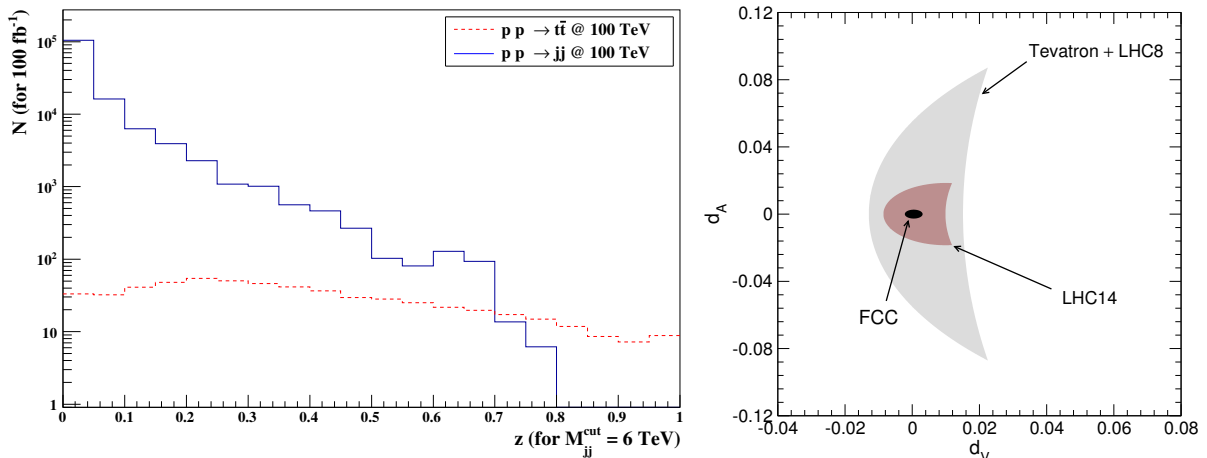


Figure 1. *Left:* distributions of the z variable of Eq. (1) for proton-proton collisions at $\sqrt{s} = 100$ TeV. We present predictions for top-antitop (red dashed) and multijet (blue plain) production, after selecting events as described in the text. We have fixed M_{jj}^{cut} to 6 TeV and normalized the results to 100 fb^{-1} . *Right:* constraints on the top dipole moments derived from measurements at the Tevatron and the LHC (gray), and from predictions at the LHC (red, $\sqrt{s} = 14$ TeV) and the FCC (black, $M_{jj}^{\text{cut}} = 10$ TeV).

2. Top pair production in 100 TeV proton-proton collisions

The top quark pair-production cross section for proton-proton collisions at $\sqrt{s} = 100$ TeV reaches 29.4 nb at the next-to-leading order accuracy in QCD, as calculated with MADGRAPH5_aMC@NLO [4] and the NNPDF 2.3 set of parton densities [5]. A very large number of $t\bar{t}$ events are thus expected to be produced for integrated luminosities of several ab^{-1} , with a significant number of them featuring a top-antitop system whose invariant-mass lies in the multi-TeV range. Whereas kinematical regimes never probed up to now will become accessible, standard $t\bar{t}$ reconstruction techniques may not be sufficient to observe such top quarks that are highly boosted, with a transverse momentum (p_T) easily exceeding a few TeV. In addition, it is not clear how current boosted top tagging techniques, developed in the context of the LHC, could be applied. Consequently, it could be complicated to distinguish a signal made of a pair of highly boosted top quarks from the overwhelming multijet background.

To demonstrate that this task is already manageable with basic considerations [6], we have analyzed, by means of the MADANALYSIS 5 package [7], leading-order hard-scattering events simulated with MADGRAPH5_aMC@NLO and matched to the parton showering and hadronization algorithms included in PYTHIA 8 [8]. We have considered, in our analysis, jets with a $p_T > 1$ TeV that have been reconstructed with FASTJET [9] and an anti- k_T jet algorithm with a radius parameter $R = 0.2$ [10]. We preselect events featuring at least two jets with a pseudorapidity $|\eta| < 2$ and at least one muon lying in a cone of $R = 0.2$ of any of the selected jets. The invariant mass of the system comprised of the two leading jets is additionally constrained to be larger than a threshold M_{jj}^{cut} . We then investigate the properties of the selected muons relatively to those of the related jet. In this context, we present on Figure 1 (left) the distribution in a z variable defined as the ratio of the muon transverse momentum $p_T(\mu_i)$ to the corresponding jet transverse momentum $p_T(j_i)$, maximized over the n final-state muons of the event,

$$z \equiv \max_{i=1,\dots,n} \frac{p_T(\mu_i)}{p_T(j_i)}. \quad (1)$$

Muons arising from multijet events are mostly found to carry a small fraction of the jet transverse momentum, which is inferred by their production mechanism (B - and D -meson decays). This

Table 1. Values of the z^{cut} parameter for different M_{jj}^{cut} choices. We also present the corresponding S/B ratio and the luminosity $\mathcal{L}_{5\sigma}$ necessary for a 5σ extraction of a $t\bar{t}$ signal from the multijet background.

M_{jj}^{cut}	z^{cut}	S/B	$\mathcal{L}_{5\sigma}$
6 TeV	0.5	0.39	36.1 fb $^{-1}$
10 TeV	0.5	0.74	202 fb $^{-1}$
15 TeV	0.4	0.25	2.35 ab $^{-1}$

contrasts with muons induced by prompt decays of top quarks that can gather a significant fraction of the top p_T . Imposing the z -variable to be larger than an optimized threshold z^{cut} , it becomes possible to obtain signal over background ratios S/B of order one and extract the $t\bar{t}$ signal at the 5σ level (defined by $S/\sqrt{S+B}$). We study, in Table 1, the z^{cut} value for different invariant-mass threshold M_{jj}^{cut} , and present the associated S/B ratio together with the luminosity necessary for a signal extraction at 5σ .

On Figure 1 (right), we illustrate how a measurement of the fiducial cross section related to the above selection with $M_{jj}^{\text{cut}} = 10$ TeV could be used to constrain the top chromomagnetic and chromoelectric dipole moments d_V and d_A . In our conventions, they are defined by

$$\mathcal{L} = \frac{g_s}{m_t} \bar{t} \sigma^{\mu\nu} (d_V + id_A \gamma_5) T_a t G_{\mu\nu}^a, \quad (2)$$

where g_s denotes the strong coupling, T^a the fundamental representation matrices of $SU(3)$, m_t the top mass and $G_{\mu\nu}$ the gluon field strength tensor. We have imported this Lagrangian into MADGRAPH5_aMC@NLO by using FEYNRULES [11, 12] to estimate the new physics contributions to the $t\bar{t}$ signal and extract bounds on the top dipole moments. While current limits have been derived from total rate measurements at the Tevatron and the LHC (gray), the FCC predictions with $M_{jj}^{\text{cut}} = 10$ TeV (black) correspond to 1 ab $^{-1}$ of collisions, and we have superimposed the expectation for the future LHC run at $\sqrt{s} = 14$ TeV (red) after setting $M_{jj}^{\text{cut}} = 2$ TeV and using standard top tagging efficiencies [13]. The FCC is hence expected to constrain top dipole moments to lie in the ranges $-0.0022 < d_V < 0.0031$ and $|d_A| < 0.0026$, which gets close to the reach of indirect probes like the electric dipole moment of the neutron ($|d_A| < 0.0012$ [14]) or $b \rightarrow s\gamma$ transitions ($-0.0038 < d_V < 0.0012$ [15]).

3. Flavor-changing neutral interactions of the top quark

In the Standard Model, the top flavor-changing couplings to the neutral bosons are suppressed due the unbroken QCD and QED symmetries and the GIM mechanism. Many new physics extensions however predict an enhancement of those interactions, whose hints are therefore searched for either in the anomalous decay of a $t\bar{t}$ pair, or in an anomalous single top production. An effective approach for describing those effects consists of supplementing the Standard Model Lagrangian by dimension-six operators that give rise to a basis of top anomalous couplings that can be chosen minimal [16]. Taking the example of the three operators

$$\mathcal{L} = \frac{\bar{c}_H}{\Lambda^2} \Phi^\dagger \Phi \Phi^\dagger \cdot \bar{Q}_L u_R + \frac{\bar{c}_W}{\Lambda^2} \Phi^\dagger \cdot (\bar{Q}_L T_{2k}) \sigma^{\mu\nu} u_R W_{\mu\nu}^k + \frac{\bar{c}_G}{\Lambda^2} \Phi^\dagger \cdot \bar{Q}_L \sigma^{\mu\nu} T_a u_R G_{\mu\nu}^a + \text{h.c.}, \quad (3)$$

where flavor indices are understood for clarity, we indeed observe that flavor-changing top couplings to the Higgs boson, the Z -boson and the gluon are induced after electroweak symmetry breaking. In our notation, Λ denotes the new physics scale, Φ (Q) a weak doublet of Higgs

(left-handed quark) fields and u_R a right-handed up-type quark field. Assuming the Wilson coefficients \bar{c} of order 1, current ATLAS and CMS data constrains $\Lambda \simeq 1$ TeV (4-5 TeV in the case of the \mathcal{O}_G operator) [17, 18]. A naive estimate of the FCC sensitivity to Λ can then be derived from these numbers by rescaling both the signal and background with the relevant cross sections and luminosities. Assuming 10 ab⁻¹ of 100 TeV proton-proton collisions, one finds that the LHC limits could be increased by a factor of about 20 [19].

Limits on new physics operators such as those of Eq. (3) could also be obtained in electron-positron collisions at high energies by relying, for instance, on single top production [20]. Signal and background have been simulated using the tools introduced in the previous section together with a modeling of the detector effects by Gaussian smearing. Exploitation of the kinematical configuration of the signal with a multivariate technique has then been found sufficient to extract the signal from the background and derive bounds on the anomalous top interactions, that have been translated in terms of limits on rare top decay branching ratios on Figure 2 (left).

4. Top parton density in the proton

In proton-proton collisions at $\sqrt{s} = 100$ TeV, all quarks including the top would appear essentially massless, so that it may seem appropriate to investigate processes with initial-state top quarks. While a six-flavor-number scheme (6FNS) allows for the resummation of collinear logarithms of the process scale over the top mass into a top density, this is only justified when these logarithms are large, the five-flavor-number scheme (5FNS) calculation spoiling in this case perturbative QCD. Both the 5FNS and 6FNS computations can however be consistently matched to guarantee accurate predictions for any scale. In the ACOT scheme [21], the 5FNS and 6FNS results are summed and the matching is achieved by subtracting from the top density f_t its leading logarithmic approximation f_t^0 that is already included in the 5FNS calculation,

$$\begin{aligned} \sigma(pp \rightarrow X^0) = & \left[f_t - f_t^0 \right] \otimes \left[f_{\bar{t}} - f_{\bar{t}}^0 \right] \otimes \sigma(t\bar{t} \rightarrow X^0) + \left[f_t - f_t^0 \right] \otimes f_g \otimes \sigma(tg \rightarrow X^0 t) \\ & + f_g \otimes \left[f_{\bar{t}} - f_{\bar{t}}^0 \right] \otimes \sigma(g\bar{t} \rightarrow X^0 \bar{t}) + f_g \otimes f_g \otimes \sigma(gg \rightarrow X^0 t\bar{t}) , \end{aligned} \quad (4)$$

where X^0 denotes any electrically and color neutral final state and f_g the gluon density.

Figure 2 (right) shows the production of a heavy neutral Higgs boson [22], and compare leading-order predictions in the 5FNS (blue), 6FNS (red) and ACOT scheme (black) for proton-proton collisions at $\sqrt{s} = 100$ TeV. For small Higgs masses, the subtraction of the leading logarithmic terms in Eq. (4) cancels almost entirely the 6FNS contribution, the ACOT result mostly being the 5FNS ones. In this region, the logarithms in the top mass are small so that their resummation into a top density is not justified. For larger masses, they start to play a role, although the use of the 6FNS alone still yields a large overestimation of the cross section. Predictions including top densities should consequently be matched to the 5FNS result, as also found for charged Higgs production [23], and not employed as such.

5. Conclusions

We have discussed three top physics cases that are relevant for collisions at future circular colliders. We have shown how highly massive top-antitop systems could be observed in proton-proton collisions at a center-of-mass energy of 100 TeV and further used to constrain top dipole moments. We have then sketched how constraints on top flavor-changing neutral interactions would improve both at future proton-proton and electron-positron colliders, and finally investigated the issue of the top parton density, relevant for proton-proton collisions at energies much larger than the top mass.

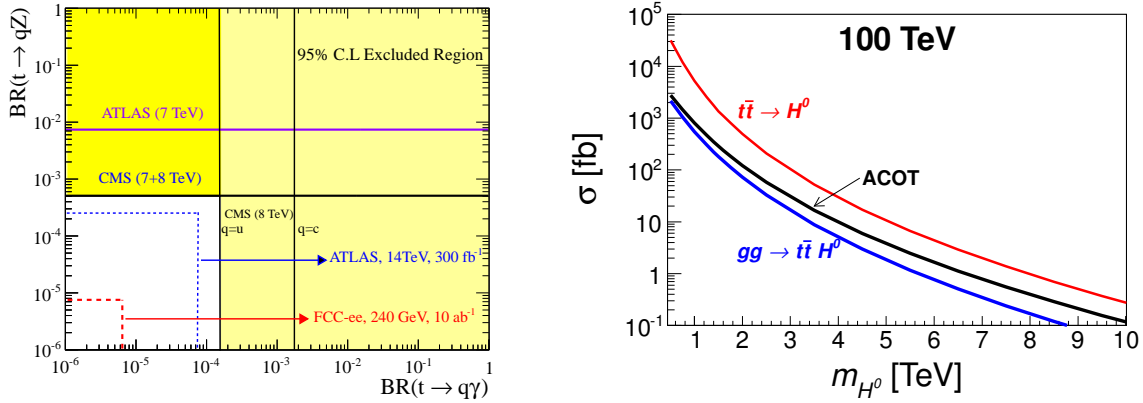


Figure 2. *Left:* limits on top decays into a neutral electroweak boson and a lighter quark. Current LHC bounds have been indicated, together with the expectation for 10 ab^{-1} of electron-positron collisions at $\sqrt{s} = 240 \text{ GeV}$. Figure taken from Ref. [20]. *Right:* Total cross section for the production of a heavy Higgs boson in the 6FNS (red), 5FNS (blue) and ACOT scheme (black) for proton-proton collisions at $\sqrt{s} = 100 \text{ TeV}$. Figure taken from Ref. [22].

Acknowledgments

I am grateful the conference organizers for setting up this very nice Top2014 event, as well as to J.A. Aguilar-Saavedra, M.L. Mangano and T. Melia for enlightening discussions on top physics at the FCC. I am also grateful to T. Han, H. Khanpour, S. Khatibi, M. Khatiri Yanehsari, M.M. Najafabadi, J. Sayre and S. Westhoff for providing material included in this report. This work has been partly supported by the LHC Physics Center at CERN (LPCC).

References

- [1] <https://espace2013.cern.ch/fcc/pages/hadron-collider.aspx>
- [2] <https://espace2013.cern.ch/fcc/pages/lepton-collider.aspx>
- [3] Bicer M *et al.* (TLEP Design Study Working Group) 2014 *JHEP* **1401** 164
- [4] Allwell J, Frederix R, Frixione S, Hirschi V, Maltoni F *et al.* 2014 *JHEP* **1407** 079
- [5] Ball R D, Bertone V, Carrazza S, Deans C S, Del Debbio L *et al.* 2013 *Nucl.Phys.* **B867** 244–289
- [6] Aguilar-Saavedra J A, Fuks B and Mangano M L in preparation
- [7] Conte E, Fuks B and Serret G 2013 *Comput.Phys.Commun.* **184** 222–256
- [8] Sjostrand T, Mrenna S and Skands P Z 2008 *Comput.Phys.Commun.* **178** 852–867
- [9] Cacciari M, Salam G P and Soyez G 2012 *Eur.Phys.J.* **C72** 1896
- [10] Cacciari M, Salam G P and Soyez G 2008 *JHEP* **0804** 063
- [11] Alloul A, Christensen N D, Degrande C, Duhr C and Fuks B 2014 *Comput.Phys.Commun.* **185** 2250–2300
- [12] Degrande C, Duhr C, Fuks B, Grellscheid D, Mattelaer O *et al.* 2012 *Comput.Phys.Commun.* **183** 1201–1214
- [13] The CMS collaboration CMS-PAS-JME-13-007
- [14] Kamenik J F, Papucci M and Weiler A 2012 *Phys.Rev.* **D85** 071501
- [15] Martinez R and Rodriguez J A 2002 *Phys.Rev.* **D65** 057301
- [16] Aguilar-Saavedra J 2009 *Nucl.Phys.* **B812** 181–204
- [17] <https://twiki.cern.ch/twiki/bin/view/atlaspublic/toppublicresults>
- [18] <https://twiki.cern.ch/twiki/bin/view/cmspublic/physicsresultsb2g>
- [19] <http://indico.cern.ch/event/284800/session/1/contribution/7/material/slides/>
- [20] Khanpour H, Khatibi S, Yanehsari M K and Najafabadi M M 2014 (*Preprint 1408.2090*)
- [21] Aivazis M, Collins J C, Olness F I and Tung W K 1994 *Phys.Rev.* **D50** 3102–3118
- [22] Han T, Sayre J and Westhoff S 2014 (*Preprint 1411.2588*)
- [23] Dawson S, Ismail A and Low I 2014 *Phys.Rev.* **D90** 014005